Ultrafast Electron−Optical Phonon Scattering and Quasiparticle Lifetime in CVD-Grown Graphene

Jingzhi Shang,[†] Ting Yu,[†,‡,*] Jianyi Lin,[§] and Gagik G. Gurzadyan[†,*]

[†]Division of Physics and Applied Physics, School of Physical and Mathematical Sciences, Nanyang Technological University, Singapore 637371, [‡]Department of Physics, Faculty of Science, National University of Singapore, Singapore 117542, and [§]Applied Catalysis, Institute of Chemical and Engineering Sciences, Singapore 62783

ABSTRACT Ultrafast quasiparticle dynamics in graphene grown by chemical vapor deposition (CVD) has been studied by UV pump/white-light probe spectroscopy. Transient differential transmission spectra of monolayer graphene are observed in the visible probe range (400−650 nm). Kinetics of the quasiparticle (*i.e.*, low-energy single-particle excitation with renormalized energy due to electron−electron Coulomb, electron−optical phonon (e-op), and optical phonon−acoustic phonon (op-ap) interactions) was monitored with 50 fs resolution. Extending the probe range to near-infrared, we find the evolution of quasiparticle relaxation channels from monoexponential e-op scattering to double exponential decay due to e-op and op-ap scattering. Moreover, quasiparticle lifetimes of mono- and randomly stacked graphene films are obtained for the probe photon energies continuously from 1.9 to 2.3 eV. Dependence of quasiparticle decay rate on the probe energy is linear for 10-layer stacked graphene films. This is due to the dominant e-op intervalley scattering and the linear density of states in the probed electronic band. A dimensionless coupling constant *W* is derived, which characterizes the scattering strength of quasiparticles by lattice points in graphene.

KEYWORDS: graphene · femtosecond spectroscopy · electron−phonon interaction · quasiparticle lifetime

Quasiparticle dynamics in graphene has attracted a great interest in the community of fundamental research and practical applications such as nanoelectronics,[1] transparent electrodes,[2] and spintronic devices.[3] Owing to the unique electronic structure, charged carriers in graphene behave like massless Dirac fermions at Fermi velocity (~10^6 m/s).[4] Investigation of these quasiparticles is critically important for the design and fabrication of graphene-based electronic devices. Since 2008, ultrafast studies[5−17] of quasiparticle dynamics in photoexcited graphene have made much progress by using pump−probe[5−16] and *Z*-scan spectroscopic methods.[16,17] In general, four kinds of graphene samples including epitaxial graphene on SiC (graphene/SiC),[5−10,17] exfoliated graphene,[11,12] graphene grown by chemical vapor deposition (CVD),[10,13,14] and graphene dispersion[16] have been used. Among these samples,[5−11,14−17] few-layer (<5) and multiple (5−100) graphene films are mostly studied. Different kinds of graphene samples have their own limitations. In particular, for epitaxial graphene/SiC, the effect of substrate[18−20] on optical properties is complex due to the existence of doping[18,19] and strain[20] near the graphene/SiC interface. For non-single-layer exfoliated graphene films, their electronic structures are different from that of the single-layer (1 L) graphene, the most promising 2D material, due to the interlayer coupling. Though there is no influence of a substrate for graphene suspension, the impact of sample uniformity and the solution environment could inevitably complicate the essential nature of quasiparticle dynamics of graphene. Until now, most of the ultrafast measurements were performed in infrared (IR)[5,6,9−11,14,15] and terahertz[7,8] probe regions, and less attention has been paid to the visible range.[12,13,15] Moreover, dependence of quasiparticle decay rate on the probe energy in graphene has not been studied in detail by ultrafast time-resolved spectroscopy.

In this paper, quasiparticle dynamics in CVD-grown graphene samples were studied in the visible region by using differential transmission ($\Delta T/T$) spectroscopy. For sample preparation, large-area monolayer graphene was grown on copper foil by CVD and then transferred onto quartz substrate;[22] multilayer graphene samples were prepared by transferring and stacking monolayer graphene one sheet by another. UV pump/white-light probe setup was employed to record the transient $\Delta T/T$ spectra and determine quasiparticle lifetimes. For monolayer and stacked samples, decay times due to electron−optical phonon (e-op) scattering are similar for the probe wavelengths from 550 to 670 nm (2.25−1.85 eV). When

* Address correspodence to yuting@ntu.edu.sg, gurzadyan@ntu.edu.sg.

Received for review February 1, 2011 and accepted March 10, 2011.

Published online March 10, 2011
10.1021/nn200419z

© 2011 American Chemical Society

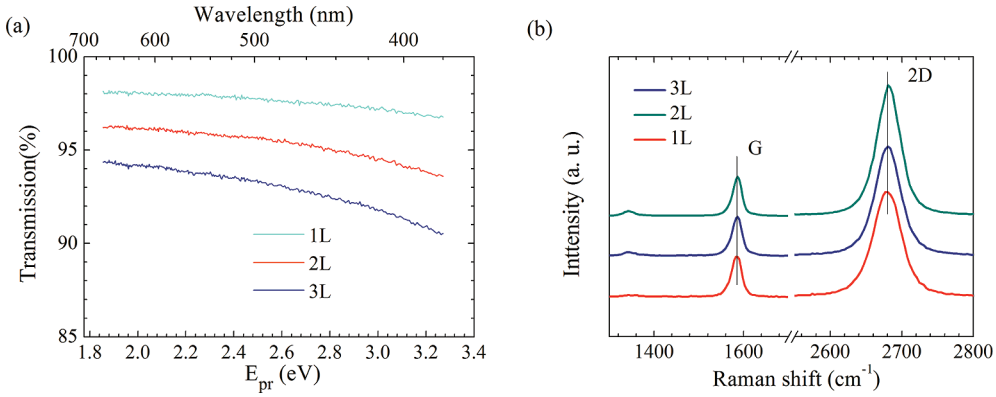

Figure 1. (a) Steady-state transmission spectra and (b) Raman spectra of 1−3 L graphene films on quartz substrates. The spectra in (b) have been normalized by the intensity of G mode.

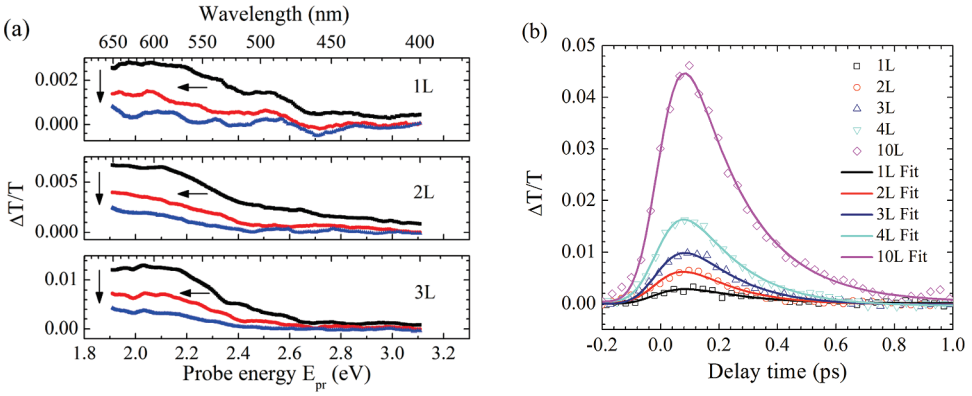

Figure 2. (a) Transient $\Delta T/T$ spectra of 1−3 L graphene films (λ_{exc} = 350 nm) at pump−probe delay times of 0.05 ps (black), 0.15 ps (red), and 0.25 ps (blue); (b) $\Delta T/T$ kinetics for 1−4 L and 10 L stacked graphene films at 610 nm.

the probe photon wavelengths vary from visible to near-IR ranges, the decay of the positive signal evolves from mono- to two-exponential kinetics and the optical phonon−acoustic phonon (op-ap) scattering rises up in the near-IR region. Fitting the energy dependence of the inverse quasiparticle lifetime, we extract a dimensionless coupling constant W,[23,24] which represents the scattering strength of quasiparticles by lattice points in graphene. The origin of the dependence of the inverse quasiparticle lifetime on energy is also identified.

RESULTS AND DISCUSSION

Figure 1a shows the steady-state transmission spectra of 1−3 L graphene samples. According to Beer's law

$$A = n\alpha = -\ln(T) \quad (1)$$

where A and n are the absorbance and the number of layers, respectively, we estimate the attenuation coefficient α to be 0.021 at 550 nm. It is close to the theoretical value of 0.023,[25] which implies that the transfer procedure for few layers does not introduce noticeable change to α. Besides, the transmittance is not constant within the whole visible range. The drop in the high energy range (>3 eV) is mainly due to the nonlinear electronic spectrum, especially the flat energy dispersion near the M point.[26] Compared with the multilayer graphene on SiC[5−10,17] or the exfoliated graphene from graphite films,[11,12] the stacked samples are expected to possess much weaker interlayer coupling. In other words, the nature of the stacked graphene films used here should be close to that of the monolayer graphene. To confirm this assumption, Raman scattering measurements have been carried out and the spectra are shown in Figure 1b. The spectra of 1−3 L stacked graphene sheets show similar characteristics of single Lorentz G (~1586 cm^{-1}) and G′ or 2D (~2680 cm^{-1}) bands,[27] which indicates the decoupling of the layers in the stacked samples.

By using pump−probe setup, transient $\Delta T/T$ spectra of 1−3 L graphene films were obtained and are shown in Figure 2a. The spectra from these three samples show similar temporal progression in the probe region. After photoexcitation at 350 nm, instantly, induced increase of the transmission was detected in the visible range. Later, $\Delta T/T$ decays and the carrier energy distribution shifts to the low-energy region accordingly. As expected, $\Delta T/T$ increases with the number of graphene layers. Figure 2b presents $\Delta T/T$ dynamics for

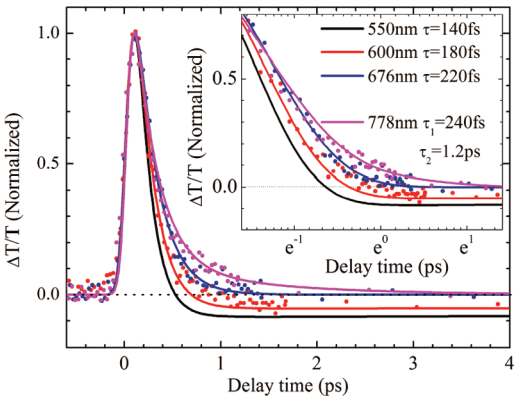

Figure 3. $\Delta T/T$ kinetics for 4 L stacked graphene films at 550, 600, 676, and 778 nm. Inset: enlarged scale.

1−4 L and 10 L graphene samples at the probe wavelength of 610 nm (2.03 eV). Being analogous to the spectral data, the intensity of $\Delta T/T$ also varies with the number of layers. Deconvolution fitting was carried out for all curves, where the rise time was refined by referring to the cross-correlation function (110 ± 20 fs) and the decay time was fitted by a monoexponential function. The positive change of transmission is due to the absorption saturation of the direct optical transition after photoexcitation. The obtained rise and decay times are 60 ± 20 and 150−200 fs, respectively. The rise time originates from the electron−electron (e-e) scattering and the initial phonon-involved scattering, while the decay time is caused by the e-op scattering, as reported.[15,21] There is no apparent dependence of the rise and decay times on the number of layers. These findings indicate that carrier relaxation processes in monolayer and stacked graphene samples are akin to each other.

Figure 3 shows $\Delta T/T$ of 4 L stacked graphene as a function of time delay, where the wavelength dependence of carrier dynamics was studied. Mono- and biexponential functions were used for fitting in visible and nearby IR regions, respectively. While probing from 550 to 676 nm, the $\Delta T/T$ kinetics reveal a monotonic increase of the decay times from 140 to 220 fs and a recovery of a negative tail because of the band renormalization by the electron−hole plasma.[21] Between 685 and 715 nm, $\Delta T/T$ signals were interfered with by a strong signal caused by the second-order frequency of the pump pulse. In the probe region between 720 to 780 nm (1.72−1.59 eV), the decay curves can be well fitted biexponentially. For the probe wavelength of 778 nm (Figure 3), the fast decay occurs with τ_1 = 240 fs due to e-op scattering; the slow decay occurs with τ_2 = 1.2 ps, which is attributed to the hot optical phonon relaxation by op-ap scattering, in agreement with the recent measurements probing at 780 nm (ref 9) and 800 nm.[14]

Figure 4a shows rise and decay times as a function of the probe photon energy E_{pr} for different layer graphene samples. By increasing the photon energies from 1.9 to 2.3 eV, decay times range from 200 ± 50 to 75 ± 25 fs and the rise times are around 60 ± 20 fs for all samples. It should be noted that the dependence of the decay time on the probe photon energy becomes apparent for the 10 L stacked graphene. The corresponding decay rate $k = 1/\tau_{decay}$ *versus* the relative electron energy $\varepsilon = E - E_f$ (E_f is Fermi energy) is plotted in Figure 4b. According to the symmetric band structure, $\varepsilon = E_{pr}/2$. Dependence of the quasiparticle decay rate *versus* ε can be well fitted by a linear function. It should be mentioned that Ando *et al.*[23,24] have theoretically predicted linear dependence of the inverse lifetime of the quasiparticle *versus* ε being mainly due to the zone-boundary optical phonon scattering in graphene:

$$\frac{1}{\tau} = \frac{2\pi}{\hbar}|\varepsilon|W \qquad (2)$$

Here $W = \langle n_i u_i^2 \rangle / 4\pi\gamma^2$ is the dimensionless coupling constant,[24] n_i is the concentration of scatterers, u_i is the potential strength, and γ is the band parameter. From Figure 4b, we obtain the slope of 0.012 ± 0.003 eV^{-1} $fs^{-1}$and extract $W \approx 1.3 \times 10^{-3}$. Hence the main decay channel in the probed region is assigned to the strong e-op scattering around K and K' points or zone-boundary intervalley scattering. This assignment is further supported by others' theoretical studies,[28] where the strongest electron−phonon coupling in graphene was demonstrated to be adjacent to K point, and consistent with the band structure measurements of the epitaxial graphene[29] by angle-resolved photoemission spectroscopy (ARPES). Furthermore, it was shown that the quasiparticle lifetimes (few hundreds of femtoseconds) in graphene are larger than those (tens of femtoseconds) in graphite[30,31] in the same probe region. This difference results from the changes[32] of the electronic structure and the density of states aroused by the interlayer coupling in graphite. The slope of the decay rate *versus* ε in graphene, being proportional to the scattering strength, is also smaller than the one in graphite: 0.029 eV^{-1} fs^{-1} (ref 30) or 0.048 eV^{-1} fs^{-1} (refs 33 and 34).

There are several factors contributing to transmission change, such as the Fermi−Dirac occupancy factor, Fermi level, initial and final states.[11,17] In general, ΔT is determined by the change of interband absorption that can be estimated by the variations in the Fermi−Dirac occupation probabilities at optically coupled states in the valence band, f_e, and in the conduction band, f_h.[11] In reference to developed expressions,[17,25] the transient differential transmittance at time t is derived as

$$\Delta T(t) = \left[1 - f_h\left(-\frac{E_{pr}}{2}, t\right) + f_e\left(\frac{E_{pr}}{2}, t\right)\right](\pi\alpha) \qquad (3)$$

Here α is the fine structure constant which defines the visual transparency of graphene. For a probe photon energy E_{pr}, $f_e(E_{pr}/2)$ is proportional to $C(T_e) \times N_e \times \exp(-E_{pr}/2k_BT_e)$, where C is a function of electron

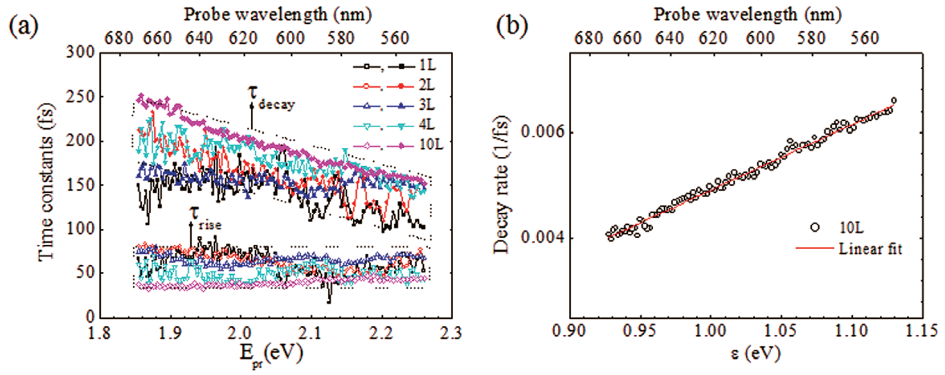

Figure 4. (a) Dependence of time constants on the probe photon energies for 1−4 L and 10 L graphene films. Errors for τ_{rise} are within ±20 fs for all samples. Errors for τ_{decay} are within ±50 fs for 1−4 L and within ±20 fs for 10 L graphene samples. (b) Decay rate *versus* ε for 10 L stacked graphene films.

temperature and N_e is the electron density.[11] Furthermore, T_e is proportional to the relative electron energy ε^{-3}, where $\varepsilon = E - E_f$. Recent calculations[45] suggest that at $T_e >$ 200−300 K optical phonon emission dominates the energy relaxation of hot Dirac fermions in graphene, which is also in agreement with our assignment in view that the measurements have been done at room temperature.

Previously, the energy dependence of the inverse quasiparticle lifetime was investigated in metals[35] and graphite,[30,31,33,36] where the e-e scattering,[35] the electron−plasmon scattering,[30] the anisotropic behavior,[31] the band structure effect,[33,35] the neutral triplet collective mode,[36] and the e-ph scattering[34,37] were considered. In graphene, the energy dependence of quasiparticle lifetime has been studied theoretically by calculating the electron self-energy[29,37−40] and unconventional dependences[37−39] are proposed, such as linear[37−39] and cubic[39] relationships. ARPES has been applied to measure this dependence in graphite[34] and graphene[4,29] by observing the relaxation of photoholes[34] below the Fermi energy. However, the calculated quasiparticle lifetimes (3−5 fs) from ARPES data are much smaller than the data measured by time-resolved spectroscopy, due to limited energy and momentum resolutions and/or high surface sensitivity.[34,40] So far, the origins of the dependences in graphite[30,33,34,36] and graphene[4] are still ambiguous, and plasmon excitation[4,30] and electron−hole pair formation[4,33,34,36] have been discussed. In this work, the observed dependence ($k \sim \varepsilon$) deviates from the conventional Fermi liquid theory[41] describing e-e scattering, where the quadratic dependence of decay rate on ε is expected in the energy band close to E_f (*i.e.*, $k \sim \varepsilon^2$).[42] For the quasiparticle energy scale of ε from 0.9 to 1.1 eV, the major relaxation channel of quasiparticle energy is the strong e-op scattering. The contribution of e-e scattering cannot be ruled out since its lifetime is beyond our time resolution (50 fs). On the basis of the above assignment of τ_{decay} and recent calculations,[23,24] the linear dependence is ascribed to the single dominant e-op decay channel and to the linear density of states in the probed electronic band of graphene.

CONCLUSION

To sum up, quasiparticle dynamics have been studied by using femtosecond differential transmission spectroscopy. Transient $\Delta T/T$ spectra of monolayer graphene were obtained in the visible region. Rise and decay kinetics of $\Delta T/T$ for monolayer were found to be similar to those of stacked samples. While passing from visible to IR probe ranges, the decay channels evolve from mono- to biexponential processes. The energies of quasiparticles mainly dissipate by e-op scattering in the visible range (550−670 nm) and both e-op and op-ap scatterings at 720−780 nm. Observed quasiparticle lifetimes decrease from 200 ± 50 to 75 ± 25 fs for E_{pr} from 1.9 to 2.3 eV. In contrast to the conventional Fermi liquid theory,[41,42] which considers only e-e interaction, an unambiguous linear energy dependence of quasiparticle decay rate was found in graphene due to e-op interaction. A dimensionless coupling constant W of 1.3×10^{-3} was evaluated, which characterizes scattering strength of quasiparticles by lattice points in graphene. The origin of the dependence of quasiparticle decay rate on energy is designated to the predominant e-op intervalley scattering and the linear density of states in the probe region, whereas ARPES data include electron−phonon as well as electron−electron and electron−plasmon interactions.

METHODS

Graphene was grown on copper foil by using low-pressure CVD.[43] Before the surface-catalyzed growth, the copper substrate was annealed at 1000 °C for 20 min where H_2 was used to remove surface oxide layers with a flow rate of 10 sccm. After that, 40 sccm methane was introduced as carbon source. Monolayer graphene on high-purity (99.999%) copper foil was obtained at 1000 °C under a chamber pressure of 3.6 Torr. Then

the sample was transferred as described in a previous report.[22] The aqueous solution of iron nitride $(FeNO_3)_3$ was employed to etch copper foil and isolate graphene monolayer. Later, the graphene film was transferred into deionized water to rinse for several times. Subsequently, quartz substrate was used to lift up the graphene films layer by layer. In this work, 1−4 L and 10 L graphene films were transferred onto quartz. All spectroscopic measurements were performed with graphene on the quartz substrate.

Steady-state transmission spectra were determined by a UV−vis spectrophotometer (Cary 100Bio, Varian) at 1.0 nm resolution. A Raman system (CRM 200, WITec) with an excitation source of diode-pumped double-frequency Nd:YAG laser (532 nm) was used for recording Raman spectra. The laser power was kept below 0.1 mW to avoid the heat-induced deformation of the sample. The Raman spectrum was calibrated by adjusting the first-order Raman peak position of a standard Si substrate to 520 cm^{-1}.

For pump−probe measurements, the output of titanium: sapphire (Legend Elite, Coherent) regenerative amplifier seeded by an oscillator (Micra, Coherent) was used as a pulse laser source: wavelength 800 nm, pulse width 80 fs, pulse repetition rate 1 kHz, and average power 3.5 W. The main part, 90%, of the radiation was converted into the UV (350 nm) by use of optical parametric oscillator (Topas, Light Conversion) with following second- and fourth-harmonic generation; this radiation was used as pump beam. The remaining 10% was used to generate white-light continuum in a CaF_2 plate (*i.e.*, probe beam). Pump pulses were focused on the sample with a lens of 30 cm focal length and an incidence angle of 10°. Probe pulses with variable time delays relative to pump pulses were used to measure time-resolved transient transmission produced by the pump pulses. The white-light continuum was split into two beams (signal and reference) and, after propagating through the sample, directed into two diode arrays attached to the spectrometers (Model 77400, Oriel). The entire setup was controlled by a computer with the help of software (LabView, National Instruments). For obtaining the transient $\Delta T/T$ spectra, chirp correction was carried out by utilizing the coherent artifact signals from the quartz substrate.[44] The experimental data were fitted to a multiexponential decay function convoluted with the instrument response function $B(t - t_0)$ centered at t_0:

$$\Delta T(t) = \int_0^\infty \left(\sum_{i=1}^{n} \Delta T_i \exp\left(-\frac{t'}{\tau_i} \right) \right) B(t - t' - t_0)\, dt' \quad (4)$$

Here $\Delta T(t)$ is the differential transmission at time t, and ΔT_i is the amplitude of the component with lifetime τ_i. The fwhm of the pump−probe cross-correlation signal in quartz was 110 ± 20 fs for the visible region.

Acknowledgment. We are grateful to Professor Maria-Elisabeth Michel-Beyerle for stimulating discussions and continuous support. J.S. thanks Dr. Lei Liu, Mr. Zhiqiang Luo, Dr. Xiaofeng Fun, and Mr. Jiaxu Yan for their helpful discussion about the dependence of the inverse lifetime on the energy. T.Y. thanks the Singapore National Research Foundation under NRF Award No. NRF-RF2010-07 and MOE Tier 2 MOE2009-T2-1-037 for support.

REFERENCES AND NOTES

1. Westervelt, R. M. Graphene Nanoelectronics. *Science* **2008,** *320*, 324–325.
2. Kim, K. S.; Zhao, Y.; Jang, H.; Lee, S. Y.; Kim, J. M.; Kim, K. S.; Ahn, J.-H.; Kim, P.; Choi, J.-Y.; Hong, B. H. Large-Scale Pattern Growth of Graphene Films for Stretchable Transparent Electrodes. *Nature* **2009,** *457*, 706–710.
3. Wu, Y. H.; Yu, T.; Shen, Z. X. Two-Dimensional Carbon Nanostructures: Fundamental Properties, Synthesis, Characterization, and Potential Applications. *J. Appl. Phys.* **2010,** *108*, 071301.
4. Bostwick, A.; Ohta, T.; Seyller, T.; Horn, K.; Rotenberg, E. Quasiparticle Dynamics in Graphene. *Nat. Phys.* **2007,** *3*, 36–40.
5. Dawlaty, J. M.; Shivaraman, S.; Chandrasekhar, M.; Rana, F.; Spencer, M. G. Measurement of Ultrafast Carrier Dynamics in Epitaxial Graphene. *Appl. Phys. Lett.* **2008,** *92*, 042116.
6. Sun, D.; Wu, Z.-K.; Divin, C.; Li, X. B.; Berger, C.; de Heer, W. A.; First, P. N.; Norris, T. B. Ultrafast Relaxation of Excited Dirac Fermions in Epitaxial Graphene Using Optical Differential Transmission Spectroscopy. *Phys. Rev. Lett.* **2008,** *101*, 157402.
7. George, P. A.; Strait, J.; Dawlaty, J.; Shivaraman, S.; Chandrashekhar, M.; Rana, F.; Spencer, M. G. Ultrafast Optical-Pump Terahertz-Probe Spectroscopy of the Carrier Relaxation and Recombination Dynamics in Epitaxial Graphene. *Nano Lett.* **2008,** *8*, 4248–4251.
8. Choi, H.; Borondics, F.; Siegel, D. A.; Zhou, S. Y.; Martin, M. C.; Lanzara, A.; Kaindl, R. A. Broadband Electromagnetic Response and Ultrafast Dynamics of Few-Layer Epitaxial Graphene. *Appl. Phys. Lett.* **2009,** *94*, 172102.
9. Huang, L.; Hartland, G. V.; Chu, L. Q.; Luxmi; Feenstra, R. M.; Lian, C.; Tahy, K.; Xing, H. Ultrafast Transient Absorption Microscopy Studies of Carrier Dynamics in Epitaxial Graphene. *Nano Lett.* **2010,** *10*, 1308–1313.
10. Wang, H.; Strait, J. H.; George, P. A.; Shivaraman, S.; Shields, V. B.; Chandrashekhar, M.; Hwang, J.; Rana, F.; Spencer, M. G.; Ruiz-Vargas, C. S.; *et al.* Ultrafast Relaxation Dynamics of Hot Optical Phonons in Graphene. *Appl. Phys. Lett.* **2010,** *96*, 081917.
11. Newson, R. W.; Dean, J.; Schmidt, B.; van Driel, H. M. Ultrafast Carrier Kinetics in Exfoliated Graphene and Thin Graphite Films. *Opt. Express* **2009,** *17*, 2326–2333.
12. Mak, K. F.; Lui, C. H.; Heinz, T. F. Measurement of the Thermal Conductance of the Graphene/SiO_2 Interface. *Appl. Phys. Lett.* **2010,** *97*, 221904.
13. Bao, Q.; Zhang, H.; Ni, Z.; Wang, Y.; Polavarapu, L.; Loh, K. P.; Shen, Z. X.; Xu, Q. H.; Tang, D. Y. Monolayer Graphene as Saturable Absorber in Mode-Locked Laser. *Nano Res.* **2010**arXiv:1007.2243v2.
14. Zou, X.; Zhan, D.; Fan, X.; Lee, D.; Nair, S. K.; Sun, L.; Ni, Z. H.; Luo, Z.; Liu, L.; Yu, T.; *et al.* Ultrafast Carrier Dynamics in Pristine and $FeCl_3$-Intercaleted Bilayer Graphene. *Appl. Phys. Lett.* **2010,** *97*, 141910.
15. Shang, J.; Luo, Z.; Cong, C.; Lin, J.; Yu, T.; Gurzadyan, G. G. Femtosecond UV-Pump/Visible-Probe Measurements of Carrier Dynamics in Stacked Graphene Films. *Appl. Phys. Lett.* **2010,** *97*, 163103.
16. Kumar, S.; Anija, M.; Kamaraju, N.; Vasu, K. S.; Subrahmanyam, K. S.; Sood, A. K.; Rao, C. N. R. Femtosecond Carrier Dynamics and Saturable Absorption in Graphene Suspensions. *Appl. Phys. Lett.* **2009,** *95*, 191911.
17. Xing, G.; Guo, H.; Zhang, X.; Sum, T. C.; Huan, C. H. A. The Physics of Ultrafast Saturable Absorption in Graphene. *Opt. Express* **2010,** *18*, 4564.
18. Varchon, F.; Feng, R.; Hass, J.; Li, X.; Nguyen, B. N.; Naud, C.; Mallet, P.; Veuillen, J.-Y.; Berger, C.; Conrad, E. H.; Magaud, L. Electronic Structure of Epitaxial Graphene Layers on SiC: Effect of the Substrate. *Phys. Rev. Lett.* **2007,** *99*, 126805.
19. Zhou, S. Y.; Gweon, G.-H.; Fedorov, A. V.; First, P. N.; de Heer, W. A.; Lee, D.-H.; Guinea, F.; Castro Neto, A. H.; Lanzara, A. Substrate-Induced Bandgap Opening in Epitaxial Graphene. *Nat. Mater.* **2007,** *6*, 770–775.
20. Ferralis, N.; Maboudian, R.; Carraro, C. Evidence of Structural Strain in Epitaxial Graphene Layers on 6H-SiC(0001). *Phys. Rev. Lett.* **2008,** *101*, 156801.
21. Breusing, M.; Ropers, C.; Elsaesser, T. Ultrafast Carrier Dynamics in Graphite. *Phys. Rev. Lett.* **2009,** *102*, 086809.
22. Li, X.; Zhu, Y.; Cai, W.; Borysiak, M.; Han, B.; Chen, D.; Piner, R. D.; Colombo, L.; Ruoff, R. S. Transfer of Large-Area Graphene Films for High-Performance Transparent Conductive Electrodes. *Nano Lett.* **2009,** *9*, 4359–4363.
23. Suzuura, H.; Ando, T. Electron Lifetime due to Optical-Phonon Scattering in a Graphene Sheet. *J. Phys.: Conf. Ser.* **2009,** *150*, 022080.
24. Ando, T. Zero-Mode Anomalies of Massless Dirac Electron in Graphene. *J. Appl. Phys.* **2010** in press.
25. Nair, R. R.; Blake, P.; Grigorenko, A. N.; Novoselov, K. S.; Booth, T. J.; Stauber, T.; Peres, N. M. R.; Geim, A. K. Fine Structure Constant Defines Visual Transparency of Graphene. *Science* **2008,** *320*, 1308.

26. Fei, Z.; Shi, Y.; Pu, L.; Gao, F.; Liu, Y.; Sheng, L.; Wang, B.; Zhang, R.; Zheng, Y. High-Energy Optical Conductivity of Graphene Determined by Reflection Contrast Spectroscopy. *Phys. Rev. B* **2008,** *78*, 201402.
27. Ni, Z.; Wang, Y.; Yu, T.; Shen, Z. Raman Spectroscopy and Imaging of Graphene. *Nano. Res.* **2008,** *1*, 273–291.
28. Richter, M.; Carmele, A.; Butscher, S.; Bücking, N.; Milde, F.; Kratzer, P.; Scheffler, M.; Knorr, A. Two-Dimensional Electron Gases: Theory of Ultrafast Dynamics of Electron–Phonon Interactions in Graphene, Surfaces, and Quantum Wells. *J. Appl. Phys.* **2009,** *105*, 122409.
29. Zhou, S. Y.; Siegel, D. A.; Fedorov, A. V.; Lanzara, A. Kohn Anomaly and Interplay of Electron–Electron and Electron–Phonon Interactions in Epitaxial Graphene. *Phys. Rev. B* **2008,** *78*, 193404.
30. Xu, S.; Cao, J.; Miller, C. C.; Mantell, D. A.; Miller, R. J. D.; Gao, Y. Energy Dependence of Electron Lifetime in Graphite Observed with Femtosecond Photoemission Spectroscopy. *Phys. Rev. Lett.* **1996,** *76*, 483–486.
31. Moos, G.; Gahl, C.; Fasel, R.; Wolf, M.; Hertel, T. Anisotropy of Quasiparticle Lifetimes and the Role of Disorder in Graphite from Ultrafast Time-Resolved Photoemission Spectroscopy. *Phys. Rev. Lett.* **2001,** *87*, 267402.
32. Partoens, B.; Peeters, F. M. From Graphene to Graphite: Electronic Structure around the K Point. *Phys. Rev. B* **2006,** *74*, 075404.
33. Spataru, C. D.; Cazalilla, M. A.; Rubio, A.; Benedict, L. X.; Echenique, P. M.; Louie, S. G. Anomalous Quasiparticle Lifetime in Graphite: Band Structure Effects. *Phys. Rev. Lett.* **2001,** *87*, 246405.
34. Sugawara, K.; Sato, T.; Souma, S.; Takahashi, T.; Suematsu, H. Anomalous Quasiparticle Lifetime and Strong Electron–Phonon Coupling in Graphite. *Phys. Rev. Lett.* **2007,** *98*, 036801.
35. Campillo, I.; Silkin, V. M.; Pitarke, J. M.; Chulkov, E. V.; Rubio, A.; Echenique, P. M. First-Principles Calculations of Hot-Electron Lifetimes in Metals. *Phys. Rev. B* **2000,** *61*, 13484–13492.
36. Ebrahimkhas, M.; Jafari, S. A. Neutral Triplet Collective Mode as a Decay Channel in Graphite. *Phys. Rev. B* **2009,** *79*, 205425.
37. Leem, C. S.; Kim, C.; Park, S. R.; Kim, M.-K.; Choi, H. J.; Kim, C.; Kim, B. J.; Johnston, S.; Devereaux, T.; Ohta, T.; *et al.* High-Resolution Angle-Resolved Photoemission Studies of Quasiparticle Dynamics in Graphite. *Phys. Rev. B* **2009,** *79*, 125438.
38. Park, C. -H.; Giustino, F.; Cohen, M. L.; Louie, S. G. Velocity Renormalization and Carrier Lifetime in Graphene from the Electron–Phonon Interaction. *Phys. Rev. Lett.* **2007,** *99*, 086804.
39. Gonzalez, J.; Perfetto, E. Unconventional Quasiparticle Lifetime in Graphene. *Phys. Rev. Lett.* **2008,** *101*, 176802.
40. Calandra, M.; Mauri, F. Electron–Phonon Coupling and Electron Self-Energy in Electron-Doped Graphene: Calculation of Angular-Resolved Photoemission Spectra. *Phys. Rev. B* **2007,** *76*, 205411.
41. Landau, L. D. The Theory of a Fermi Liquid. *Sov. Phys. JETP* **1957,** *3*, 920.
42. Quinn, J. J.; Ferrell, R. A. Electron Self-Energy Approach to Correlation in a Degenerate Electron Gas. *Phys. Rev.* **1958,** *112*, 812.
43. Li, X.; Cai, W.; An, J.; Kim, S.; Nah, J.; Yang, D.; Piner, R.; Velamakanni, A.; Jung, I.; Tutuc, E.; *et al.* Large-Area Synthesis of High-Quality and Uniform Graphene Films on Copper Foils. *Science* **2009,** *324*, 1312–1314.
44. Dietzek, B.; Pascher, T.; Sundstrom, V.; Yartsev, A. Appearance of Coherent Artifact Signals in Femtosecond Transient Absorption Spectroscopy in Dependence on Detector Design. *Laser Phys. Lett.* **2007,** *4*, 38–43.
45. Tse, W. K.; Das Sarma, S. Energy Relaxation of Hot Dirac Fermions in Graphene. *Phys. Rev. B* **2009,** *79*, 235406.